

Resistivity Anisotropic Inclusion Model for Clastic Sediments

Michelle Ellis (RSI) and Olivier Kirstetter (REPSOL).

Summary

In this paper we propose a new rock physics workflow which uses a combination of the Hashin-Shtrikman bounds (Hashin and Shtrikman, 1962) and the Joint Self Consistent Approximation (Bruggeman, 1935; Landauer, 1952; Berryman, 1995) and Differential Effective Medium model (Bruggeman, 1935; Sen *et al.*, 1981) to estimate the horizontal and vertical resistivity of a clastic anisotropic rock. This model has been developed such that it is suitable for both sands and shales. We assume that anisotropy is caused by the collapse of the pore space as the rock is buried and the rearrangement of grains (layering and fracture induced anisotropy is not considered). The aspect ratio of the inclusions is estimated from the effective porosity of the rock. Shallow soft and stiff rocks have a more disordered microstructure and high effective porosity and therefore have high effective aspect ratios. Deep soft rocks (which are dominated by shales) have a more ordered microstructure and therefore lower aspect ratios which are aligned. Stiff deep rocks, where effective porosity is better preserved as they are buried, have higher aspect ratios. By linking the effective aspect ratio to the effective porosity we can model both sands and shales with the same model without changing the input parameters.

Introduction

Most rocks display some level of anisotropy both elastically and electrically. However electrical anisotropy can be many times greater than elastic anisotropy. Whereas we may, rightly or wrongly, assume the earth is isotropic in many cases in the seismic domain, we cannot do this in the electrical domain. Disregarding resistivity anisotropy will lead to misleading Controlled Source Electromagnetic (CSEM) survey feasibility studies, inaccurate CSEM data analysis, inaccurate estimations of hydrocarbon saturations and, consequently, erroneous interpretations (Ellis *et al.*, 2011). Therefore, models that consider and are calibrated to the both the horizontal and vertical resistivities are essential.

A further consideration is that rock physics models use is not limited to the interpretation of well log data. They maybe used for the interpretation and petrophysical inversion of geophysical data. Therefore, a model or workflow that handles the transition between different rock types is also desirable.

The model presented, aims to estimate both the vertical and horizontal resistivity of a rock for both sands and shales.

Anisotropic Rock Physics Model

The proposed rock physics workflow (Figure 1) uses a combination of the Hashin-Strickman (HS) lower bound model and the Joint Self consistent approximation and differential effective medium model (SCA/DEM).

HS bounds – This model calculates the narrowest set of bounds where one component is completely isolated and the other is fully interconnected.

SCA/DEM model – This is an inclusion type model which can estimate the effective resistivity of a 2 phase medium. The Self Consistent Approximation model (SCA) is used to estimate the effective resistivity a specified porosity (biconnected porosity point, ϕ_B). If this porosity is between 0.4 and 0.6 we assume that the effective medium is bi-connected (both phases are interconnected). The Differential Effective Medium (DEM) model (which preserves the starting medium) is then used to add and remove the small fractions of the components until the required volume fractions are obtained. This allows us to build a rock where both components are interconnected at all volume fractions.

Our workflow assumes that the rock is composed of 4 components, brine, oil/gas, clay and quartz (or another resistive grain). Similar to typical elastic rock physics workflows we estimate the effective properties of the fluids and solids separately, in this case using the HS model for both. The volume fraction of the fluid is assumed to be the effective porosity. All other fluid is associated with the clay. For the solid we assume that the quartz forms the grains and clay the cement. We now have two phases (solid and fluid) which can be passed to the anisotropic SCA/DEM model (Figure 1). The SCA/DEM model can then be used to estimate the effective resistivity of the rock. Anisotropy is induced by aligning the ellipsoidal inclusions. The model has three unknowns, clay resistivity, biconnected porosity point (ϕ_B) and aspect ratio of the inclusions. These parameters can be calibrated to data.

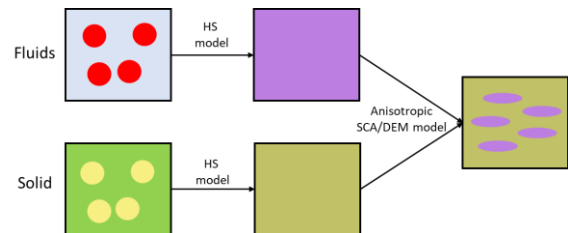


Figure 1: Workflow for the electrical anisotropic SCA/DEM

Resistivity Anisotropic Inclusion Model

Calibration of parameters

The model has been tested and calibrated against data from the Barents Sea. Ellis *et al.*, 2017 indicates that anisotropy is primarily controlled by burial and the collapse of the pore space. We therefore estimate the aspect ratio and ϕ_B that gives the best fit to well log data where the data has been binned by effective porosity regardless of facies. We

assume effective porosity decreases with burial and does not rebound with uplift (Avseth *et al.*, 2009; Revil *et al.* 2013). Figure 2 (top) shows the changes in aspect ratio with effective porosity for several wells from the Barents Sea. In each case aspect ratio decreases (causing increasing anisotropy) as porosity decreases. The best fit is a logarithmic regression. All the wells show the same pattern although there is a slight shift between wells. The fit at 7220/8-1 (Skrugard) is particularly good. The Skrugard

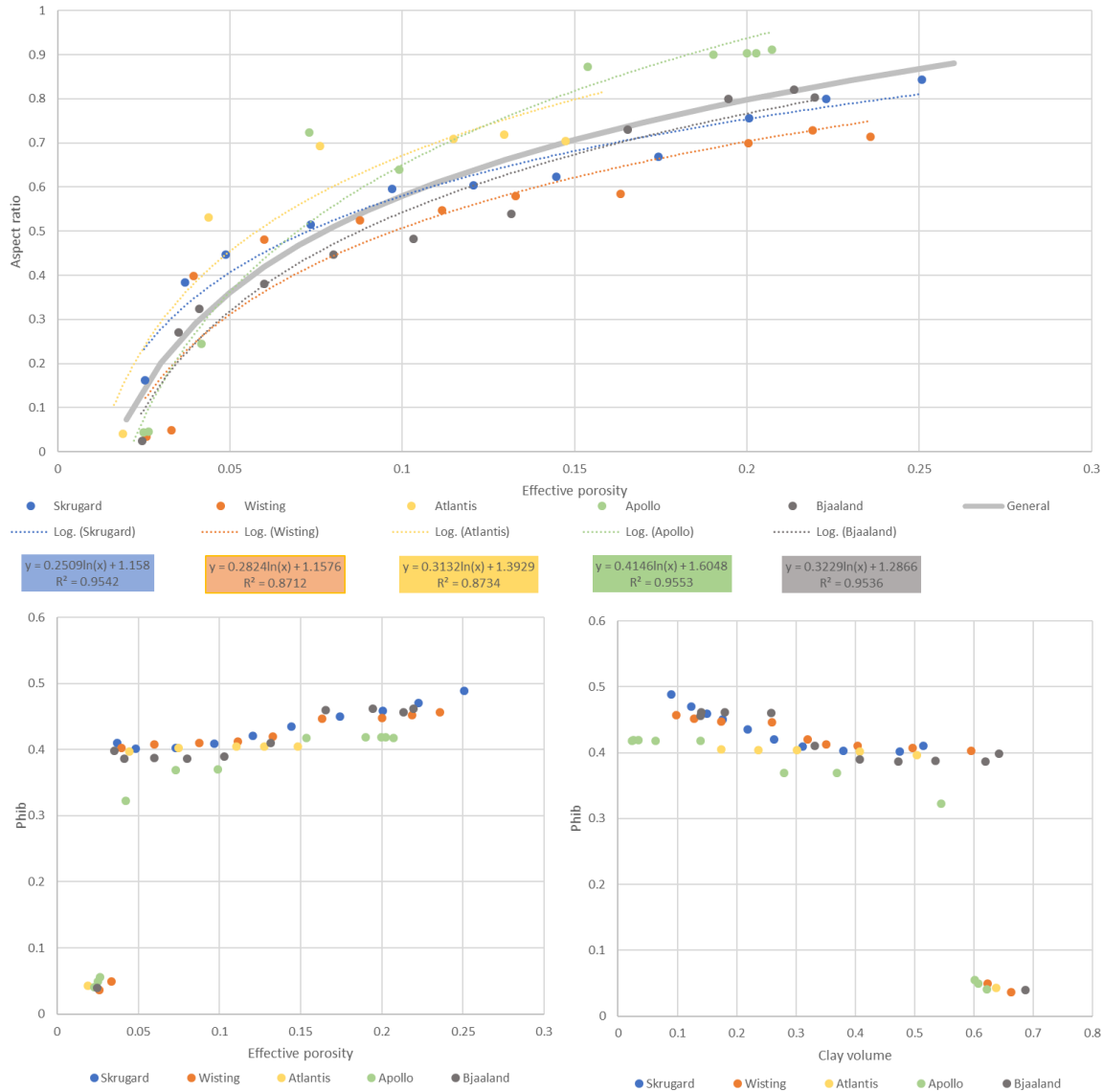


Figure 2: Top - Change in aspect ratio with effective porosity calculated using the SCA/DEM model for 5 Barents Sea Wells individually. Bottom Left - Change in ϕ_B with effective porosity. Bottom Right - Change in ϕ_B with Clay volume.

Resistivity Anisotropic Inclusion Model

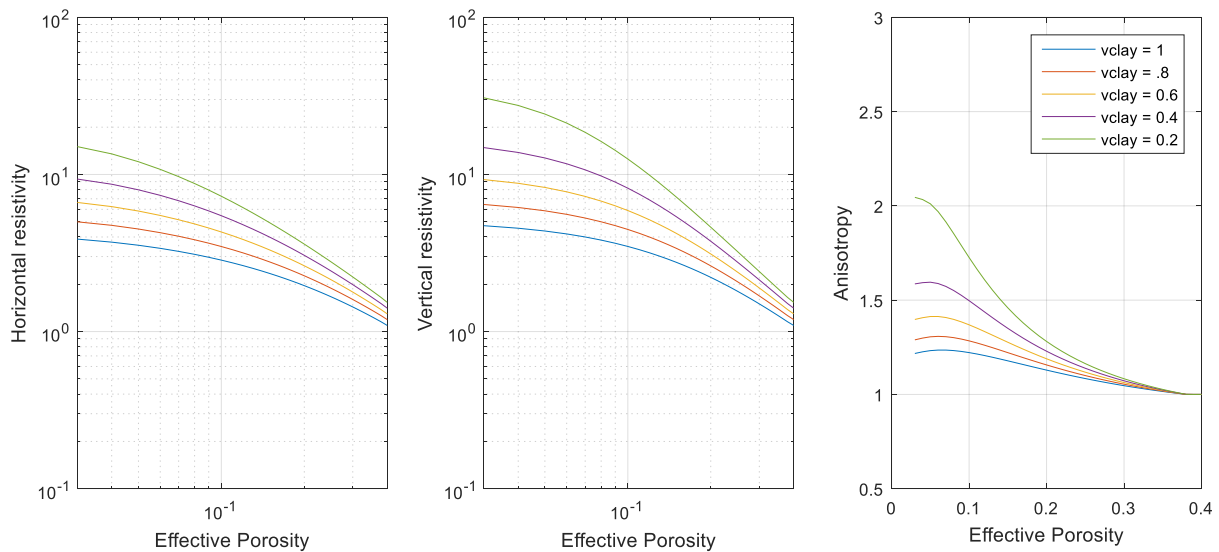


Figure 3: Change in Horizontal resistivity (Left), Vertical resistivity (Middle) and anisotropy (Right) as porosity and clay resistivity changes calculated using the general trend between effective porosity and aspect ratio given in Figure 2.

well is long with a large range of effective porosities and the lowest amount of uplift. This makes calibration in this well easier. It should, however, be noted that the Torsk and Kolmule formations were removed from the analysis because they have significantly different trends.

This trend in the data implies that both sands and shales with high effective porosity, which we would expect to see in shallower rocks, can be modelled using a high effective aspect ratio. As the rocks are buried, soft rocks (usually shales) tend to lose effective porosity as the pore space collapses and the grains align. This decreases the effective aspect ratio. Stiffer rock (often sands) lose far less effective porosity and the aspects stay high with burial. Therefore, we can use this model to estimate resistivity in both sands and shales by changing the aspect ratio with porosity.

Because the wells all behave in a similar manner, we have also created a general trend to the data. Using this trend between the effective porosity and aspect ratio we can now see that anisotropy will increase with decreasing effective porosity (Figure 3).

The required ϕ_B point was also compared to effective porosity and clay volume (Figure 3). It can be seen that ϕ_B slowly decreases as effective porosity decreases and clay volume increases. This pattern is seen until very low rock porosities are present. At this point ϕ_B drops dramatically. This indicates that at very low porosities all the porosity is isolated. A general trend can also be obtained for the biconnected porosity from all the wells.

Comparison of model with 7220/8-1

Figure 4 shows a comparison of the measured resistivity data at the Skrugard well and the results of the model using aspect ratio and ϕ_B calculated using the regression fits. The model was run twice. Once with the Skrugard specific calibration (green lines) and once with the general calibration (red lines). It can be seen that the model performs extremely well along the length of the log (although the Torsk and Kolmule formations were not included). Both sets of trends give good results. Good anisotropies were also obtained although there was less scatter compared to the measured data. The resistivities results are slightly off in the reservoir (~1280 – 1380 m), however we should note that the S_w values used in the model are estimated independently using the Simandoux model and only the horizontal resistivity. They were also clipped at 0.05. Therefore, they are not necessarily the correct values. In general, the difference between the two sets of results is very small. For the horizontal resistivity there is a small difference at low effective porosities. At all other porosities the results are very similar. For the vertical case, at low resistivities the Skrugard calibrated parameters give a slightly higher resistivity. This switches as the resistivities increase. But again, the results are very similar. This indicates that we could possibly use the same general trend for other wells within the Barents Sea.

Conclusions/Discussion

Resistivity Anisotropic Inclusion Model

The results of this model indicate the SCA/DEM model can be used for estimating the horizontal and vertical resistivities of the rock. This model has advantages over empirical model such as Simandoux because the vertical and horizontal resistivities are linked (which gives us the possibility of calibrating the model when just one resistivity direction is available). The model can be calibrated to a single well but most wells can be modelled well using a general regional trend.

The model works for both sands and shales by allowing the aspect ratio to fluctuate with effective porosity. Shallow shales and sands have high effective porosity and therefore high aspect ratios. Deeper shales with low effective

porosity have low aspect ratios and higher anisotropies. It should be noted that because of the way this model estimates aspect ratio it fits general porosity trends and does not fit some more unique formations. It also does not consider anisotropy due to fracturing or sub-resolution layering.

Acknowledgments

The authors would like to thank REPSOL and RSI for permission to present this work. It was performed under the joint BOLT project.

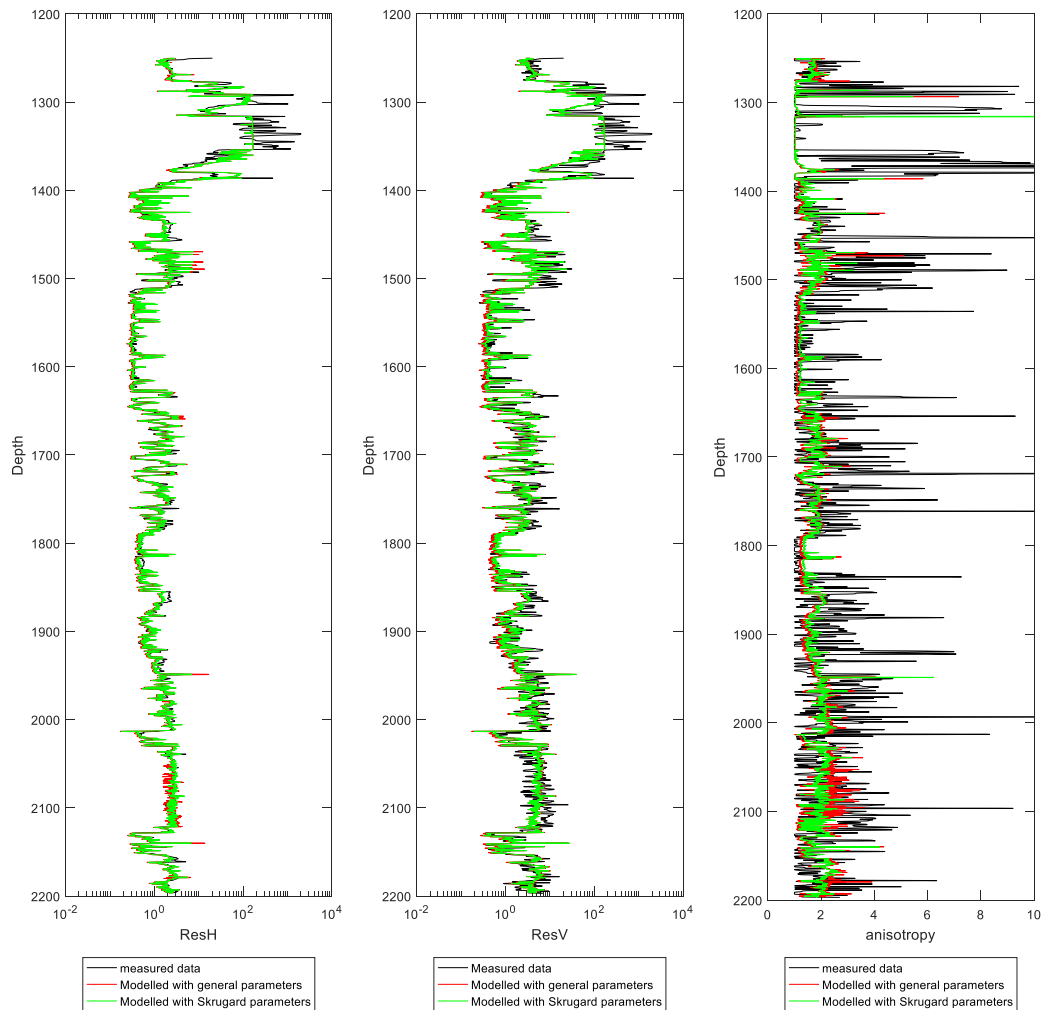


Figure 4: Comparison of measured resistivity and anisotropy with modelled data. The red lines show the results with the general trend applied and the green lines shows with the results when the Skrugard specific trend applied.